ARTICLE

Self-Assembled Growth, Microstructure, and Field-Emission High-Performance of Ultrathin Diamond Nanorods

Naigui Shang,[†,*] Pagona Papakonstantinou,[†] Peng Wang,[‡] Alexei Zakharov,[§] Umesh Palnitkar,[⊥] I-Nan Lin,[⊥] Ming Chu,[¶] and Artemis Stamboulis[¶]

[†]Nanotechnology Research Institute, School of Electrical and Mechanical Engineering, University of Ulster, Shore Road, Newtownabbey, BT37 0QB, United Kingdom, [‡]UK SuperSTEM, Daresbury Laboratory, Cheshire, WA4 4AD, United Kingdom, [§]MAX-Laboratory, Lund University, Box 118, Lund S-22100, Sweden, [⊥]Department of Physics, Tamkang University, Tamsui 251, Taiwan, Republic of China, and [¶]Department of Metallurgy and Materials, University of Birmingham, Edgbaston, Birmingham, B15 2TT, United Kingdom

ABSTRACT We report the growth of ultrathin diamond nanorods (DNRs) by a microwave plasma assisted chemical vapor deposition method using a mixture gas of nitrogen and methane. DNRs have a diameter as thin as 2.1 nm, which is not only smaller than reported one-dimensional diamond nanostructures (4—300 nm) but also smaller than the theoretical value for energetically stable DNRs. The ultrathin DNR is encapsulated in tapered carbon nanotubes (CNTs) with an orientation relation of $(111)_{diamond}//(0002)_{graphite}$. Together with diamond nanoclusters and multilayer graphene nanowires/nano-onions, DNRs are self-assembled into isolated electron-emitting spherules and exhibit a low-threshold, high current-density (flat panel display threshold: 10 mA/cm^2 at 2.9 V/μm) field emission performance, better than that of all other conventional (Mo and Si tips, *etc.*) and popular nanostructural (ZnO nanostructure and nanodiamond, *etc.*) field emitters except for oriented CNTs. The forming mechanism of DNRs is suggested based on a heterogeneous self-catalytic vapor—solid process. This novel DNRs-based integrated nanostructure has not only a theoretical significance but also has a potential for use as low-power cold cathodes.

KEYWORDS: diamond nanorods · carbon nanotube · aberration-corrected TEM · HAADF · PEEM · NEXAFS · field emission

Various carbon allotropes including fullerene, single/multiwall carbon nanotube (SWCNT/MWCNT), graphite, and diamond have received enduring attention over the last two decades because of their excellent properties and potential wide applications. Their completely different properties have been ascribed to the diversity of C—C chemical bonds (sp^1, sp^2 or sp^3). For example, sp^3 C—C bonded diamond is a wide band gap semiconductor exhibiting a combination of superior properties such as negative electron affinity, chemical inertness, high Young's modulus, the highest hardness and room-temperature thermal conductivity,[1] whereas sp^2 C—C bonded graphite is an excellent conductor and one of the softest materials in nature. Meanwhile, the dimension and size could play a critical role in determining the properties of such materials. For example, sp^2-bonded SWCNT is a unique one-dimensional (1D) material, which has not only a high aspect ratio, a high thermal conductivity, the highest tensile intensity, and Young's modulus, but also exhibits either metallic or semiconducting behavior with quantum electron transport.[2] The most convincing evidence of size effects is that the properties of thin SWCNTs are superior to those of thick MWCNTs. Thus, high aspect-ratio, nanoscale 1D diamond in the form of nanotubes, nanorods, nanowires, nanofibers, nanopillars and so on has become a hot research topic in both theoretical and experimental fields, represented as a counterpart of CNTs due to different C—C bonding nature of sp^3 *versus* sp^2. To date, many novel properties of diamond nanorods (DNRs) such as high thermal conductivity, a zero strain stiffness, *etc.* have been theoretically predicted,[3,4] foreseeing their possible use in cross-link facilitated heat transfer and thermal management systems.[5,6] The realization of vertically aligned conducting diamond nanorods arrays, which can detect picomolar concentrations of target DNA has triggered the development of sensors for clinical diagnostics, environmental sensing as well as other applications at the interface between biology and microelectronics.[7] Like SWCNTs, DNRs may be semiconducting, semimetallic or metallic, depending on their diameter, surface morphology and surface functional species. Their band gaps start to be tunable at a diameter of less than about 2.39 and 4.14 nm for the dehydrogenated and hydrogenated DNRs, respectively.[8] So far diverse 1D diamond nanostructures have been synthesized by hydrogen plasma

*Address correspondence to ngshang@hotmail.com.

Received for review February 18, 2009 and accepted March 26, 2009.

Published online April 3, 2009.
10.1021/nn900167p CCC: $40.75

post-treatment of CNTs, high-temperature, high-pressure, microwave plasma chemical vapor deposition (MPCVD), and plasma etching,[9−15] having a diameter in the range of 4−300 nm and a small aspect ratio, which are significantly different from those of SWCNTs (~1−2 nm and large aspect ratio). The synthesis of ultrathin 1D diamond nanostructures could lead to the discovery of potentially novel properties, not currently available, as was the case that had occurred previously at the initial stage of CNT studies. Meanwhile, the theoretical studies showed that DNRs are energetically stable only at the diameter range of 2.7−9 nm.[16,17] Thus, the growth of ultrathin (less than 2.7 nm), large aspect ratio DNRs is not only an experimental challenge but also has theoretical significance. In addition, most of the properties of DNRs have not been investigated fully with the majority of the studies being concentrated on theoretical predictions, whereas their experimental study is still at an infant stage. In this work, we report the MPCVD growth of 2.1 nm ultrathin DNRs, which are encapsulated in tapered CNTs with continuously variable two to five or more graphene walls. Together with the presence of a few diamond nanoclusters and graphene nanowires/nano-onions, they are all self-assembled into spherical structures. Their excellent field emission property is reported for the first time. This novel hybrid nanostructure has the potential to marry the major advantages of its individual components and to realize significant improvements in their current nanoelectronics and bioelectronics applications.

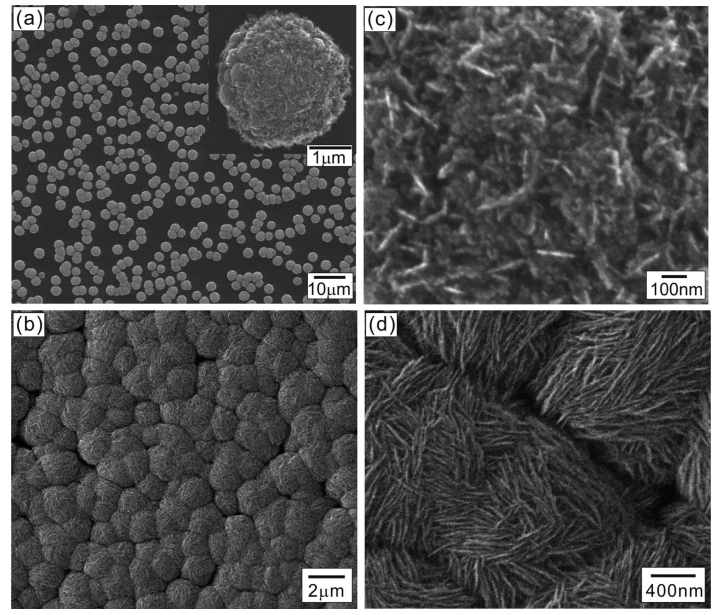

Figure 1. (a and b) Typical SEM images of isolated and continuous DNRs integrated spherules; (c and d) corresponding englarged SEM images of panels a and b.

RESULTS AND DISCUSSIONS

Figure 1a shows the scanning electron microscopy (SEM) image of DNRs deposited on Si for 30 min. It can be seen that there are many spherical structures uniformly dispersed on Si with an approximate density of $5.5 \times 10^6/cm^2$. They are either isolated with a perfect spherulus shape or some are coalesced together into irregular shapes. These sphere-shaped structures are different from those of diamond cauliflowers or diamond balls, which are made of faceted diamond crystals or carbon granules.[18] They seemingly are made of a large quantity of short and straight nanorods with a diameter of less than 20 nm and a length of less than 200 nm, together with some nanoclusters. In whole they have an appearance similar to textured radial carbon nanoflake spherules deposited on steel at low temperature and low power, as reported previously.[19] Figure 1b shows the SEM image of DNRs deposited on SiO_2/Si for 60 min. The DNR spherules are coalesced into a continuous film made of locally aligned DNRs, exhibiting a morphology similar to that of reported diamond nanowires.[12]

To further characterize its microstructure, we used both a 200 kV high-resolution transmission electron microscopy (TEM) and a 100 kV scanning transmission electron microscopy (STEM) equipped with a spherical aberration corrector, in which exclusive high-angle annular dark-field (HAADF) images can be obtained. Compared to conventional TEM, STEM not only makes it possible to see lattice fringes without intentionally selecting a specific orientation, but also directly recognizes elements due to the mechanism of atomic-number-dependent atomic scattering.[20,21] The DNR was scratched onto a holey carbon-coated Cu grid for the TEM observation. Energy dispersive X-ray spectroscopy (EDS) microprobe shows that the sample is carbon predominant. Except for Si and Cu originating from the substrate and TEM grid, respectively, no other metal elements were detected (Figure 2c). Figure 2a shows a typical low-magnification TEM image. It can be seen that there are a few nanometer sized clusters and many 50−300 long rod/cone-like 1D nanostructures. Selective area diffraction pattern (SAED) (Figure 2b) from the 1D nanostructures consists of a few reflection spots and a set of reflection rings, confirming the presence of textured graphite and polycrystalline diamond in the sample. Figure 2 panels d−g illustrate typical high resolution TEM images of the sample. Except for a few diamond nanoclusters and straight or curved, branched multilayer graphene nanowires and nano-onions, the majority of 1D nanostructures were found to be DNRs. The diamond nanoclusters are well crystalline with a (111) diamond plane spacing of 0.205−0.21 nm. The straight or curved, branched multilayer graphene nanowires/nano-onions are ordered displaying clear graphene planes with a (0002) lattice spacing of 0.337−0.367 nm. DNRs with a diameter range of 2.1−4.2 nm were found to be embedded in either an amorphous matrix or in carbon nanotubes, in agreement with the previously reported dia-

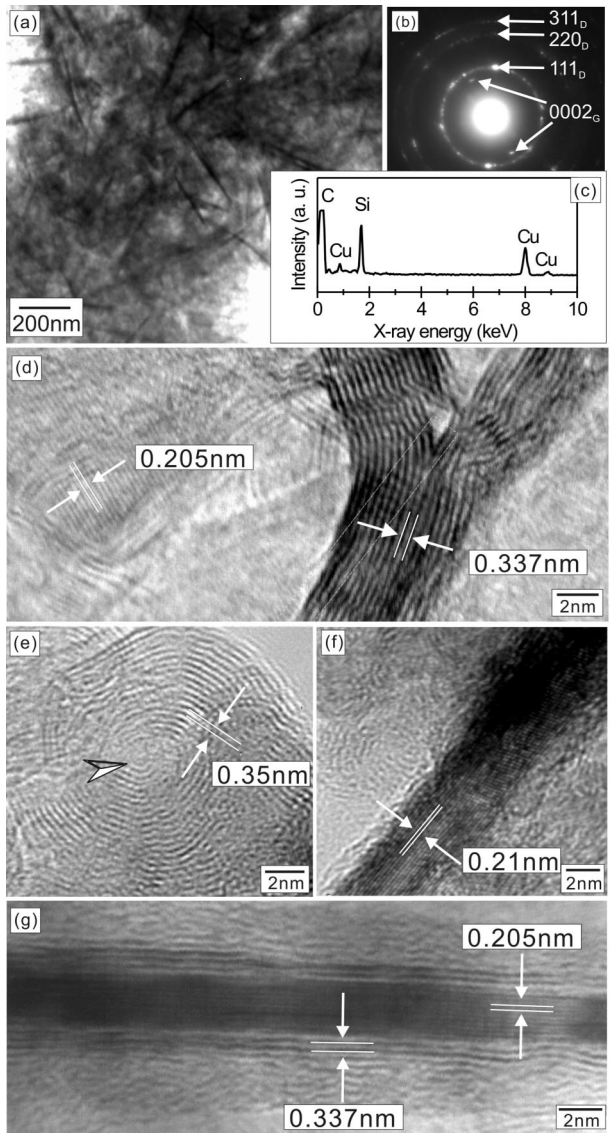

Figure 2. (a−c) Low magnification of TEM images, SAED pattern, and EDS spectrum; (d−g) high resolution TEM images showing diamond nanoclusters, graphene nanowires, and DNRs in the sample.

mond nanowires.[11] Figure 2g shows a typical image of the thinnest DNR, which is an elongated single crystal rather than a chain of several grain segments connected by multilayer graphene.[12] The diameter throughout the DNR is only 2.1 nm, which to the best of our knowledge is the thinnest ever reported 1D diamond nanostructure. This value is also smaller than the theoretically predicted diameter range of 2.7−9 nm, where DNRs are energetically stable.[16] Here, the few-layer graphene-rolled CNTs could serve as a shield for keeping the DNR at low free energy. This finding provides an insight on the growth of ultrathin diamond nanorods and could act as a trigger for stimulating future theoretical and experimental work on the DNR growth.

The study of 1D nanostructural tip is a critically interesting subject as it is relevant to the growth mechanism and material's property. Figure 3 illustrates a high magnification HAADF image of the DNR tip. Due to their different atomic density and crystalline structure, graphite and diamond exhibit different brightness and contrast in the HAADF image. Along the axial growth direction of [1$\bar{1}$0] from the tip to the root, the DNR was surrounded by a tapered carbon nanotube with gradually increasing number of graphene walls ranging from two to five or more layers. The diamond and graphite could have an epitaxial relation of $(111)_{diamond}//(0002)_{graphite}$,[22] which ensures a continuation of the flat hexagonal network of graphene on a buckled hexagonal network of diamond {111} planes. Such an epitaxial relationship could be responsible for the system's low free energy, leading to the formation of ultrathin DNRs. The tip of DNRs observed here is free of metal, graphene, and amorphous carbon and differs from the tip of diamond nanowires obtained in earlier studies, which has a fullerene-like cap at its end.[11] Thus, the tip could be terminated with H atoms, as illustrated in the following near edge X-ray absorption fine structure (NEXAFS) analysis.

X-ray photoemission energy microscopy (PEEM) is an X-ray excited nondestructive imaging technique that is able to provide spectroscopic information on a nanometer scale, working either on X-ray photoelectron spectroscopy or NEXAFS mode. Figure 4a is a typical PEEM image of the sample with a view field of 25 μm at the photon energy of 320 eV. It is clear that there are many isolated DNR constituent spherules. Figure 4b shows a C−K edge NEXAFS spectrum taken from an individual spherule. Except for a typical sp^2-bonded carbon characteristic peak at 285 eV, the NEXAFS spectrum profile of a DNR spherule is very similar to that of single crystalline diamond, which has two specific features: a diamond exciton sharp peak at 289 eV and a second absolute band gap of diamond represented by a large dip at 302.5 eV.[23] This confirms that the DNR spherule consists of predominant sp^3 diamond and sp^2 graphitic phase, in corroboration with the TEM results. In addition, there are two weak peaks located at 286.5−287.5 and 282.5 eV, which could originate from C−H bonding or localized gap states at dangling bonds and distorted sp^3-bonding sites, respectively.[24] Thus, the present spherule surface is terminated with H, leading to a negative electron affinity surface for enhancing the field emission.

The field emission measurement was carried out in a vacuum chamber with a base pressure below 10^{-6} torr at room temperature by using a diode configuration with a 2 mm diameter tungsten tip as anode. The distance between the tip and the cathode was controlled at 100 μm by a digital micrometer controller and an optical microscope.[25] Figure 5 shows the relation of emission current density as a function of applied electrical field of DNRs. The inset is the corresponding linear Fowler−Nordheim (F−N) plot, indicating that the field electron emission of NDRs follows the classic field emission mechanism. The turn-on field at the current density of 0.01 mA/cm^2 is approxi-

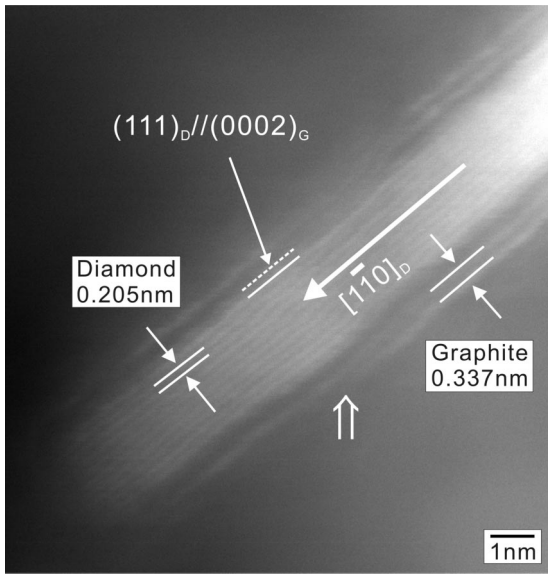

Figure 3. High magnification HAADF images of the tip of DNRs.

mately 1.3 V/μm, which is greatly less than that of many carbon nanostructures, such as tubular graphite cones, carbon nanoflake films, carbon nanotubes, and nanodiamond films.[26−28] The threshold field at an emission current density of 1 mA/cm^2 is about 1.9 V/μm, which compares favorably with respect to various nanostructural emitters, for example CNT, ZnO, CN*x*, GaAs, GaN,

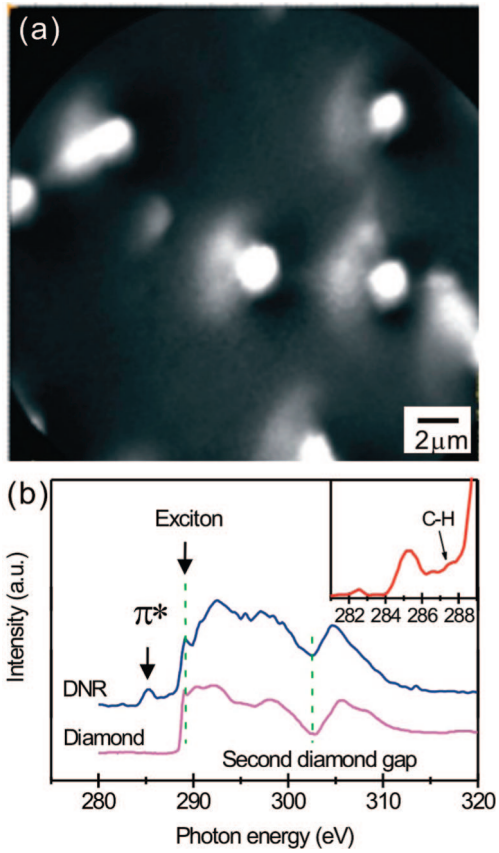

Figure 4. (a) PEEM image of the DNR sample; (b) NEXAFS spectrum taken from an individual DNR spherule.

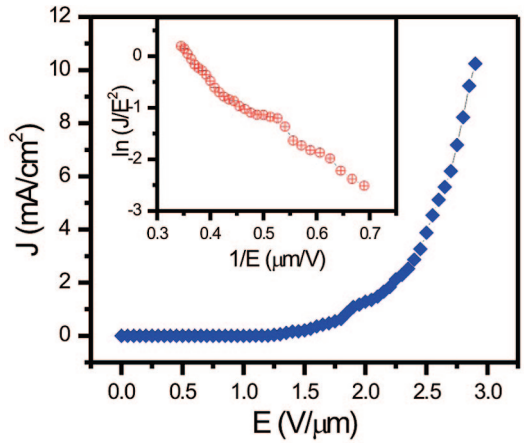

Figure 5. Emission current density as a function of applied electrical field for DNRs and corresponding F−N plot.

AlN, BCN, *etc.*[29] The threshold field at which an emission current density of 10 mA/cm^2 is achieved, being considered as a figure of merit for conventional flat panel displays, is less than 2.9 V/μm. This value is better than previously reported values for various field-emitting materials including single wall CNT, nanodiamond, and Mo and Si tips,[30−32] but worse than that of oriented high density multiwall CNTs.[33] The low turn-on field and large current density of DNRs could be assigned to the following factors: (1) isolated DNR spherules act like separated emitting tips, which not only could have a large field enhancement factor, but could also effectively depress the screen effect; (2) the presence of novel hybrid nanostructures of diamond nanocluster, DNR, CNT, and graphene nanowires/nano-onions will lead to enhanced properties, such as higher electron mobility and transport properties, derived from the combined effects of the individual constituents; (3) H-terminated DNRs have a negative electron affinity surface and a higher surface conductivity.[34,35] Additionally, it is noticeable that nitrogen in the ambient could be partially incorporated into the structure during the deposition, leading to a great change in the electronic structure and higher conductivity due to nitrogen vacancy complexes as shallow donors and grain boundary nitrogen dangling bonds or nitrogen π bond complexes as compensation centers.[12]

The growth mechanism of one-dimensional hybrid nanostructures of DNRs and CNTs is an almost unexplored subject. As we know, diamond is a metastable carbon phase and the growth of highly crystalline diamond requires a hydrogen-rich environment, where hydrogen plays an extraction role, preferentially etching amorphous carbon and graphite and enhancing diamond nucleation and growth.[1] The nanodiamond growth usually occurs in a hydrogen-free environment,[36] where Ar or N_2 gases are used to replace hydrogen and depress the growth of large diamond crystals. Up until today, many methods have been attempted to increase the diamond nucleation and growth such as

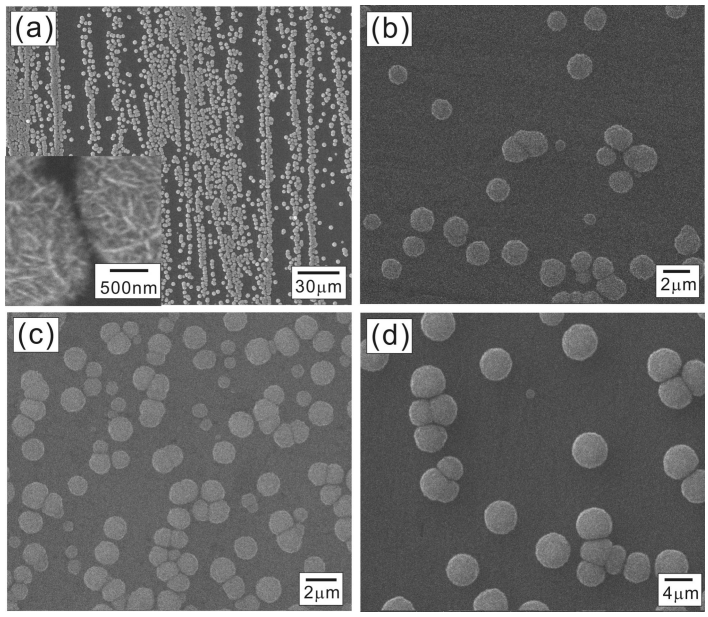

Figure 6. (a) SEM images of DNRs grown on the diamond scratched Si, showing the spherule prefer to nucleate on the scratched sites, the inset is an enlarged image; (b and c) SEM images of DNRs grown on Si and SiO_2-coated Si for 30 min; (d) SEM images of DNRs grown on Si by using a −100 V bias for 30 min.

ion bombardment, mechanical abrasion, *etc*. CNTs are a 1D nanomaterial, which usually follows a vapor−liquid−solid catalytic mechanism except for the self-catalytic or catalyst-free self-assembly growth.[37] As a metastable 1D nanostructure, DNRs can only grow in a critical condition, which should simultaneously meet both the metstable thermodynamic and 1D growth. Figure 6a shows a typical SEM image of DNR spherules grown on the Si substrate scratched by diamond particles. The DNR spherules are not uniformly dispersed on the Si surface. It is clear that the DNR spherules prefer to grow onto the scratched line. The nucleation density of DNRs is enhanced by creating denser lines. DNR spherules were absent on a non-scratched surface. This nucleation and growth behavior is consistent with that of polycrystalline CVD diamond, where either residual diamond particles or various structural defects on the surface, produced by scratching, act as nucleation sites. As another fashionable technique, ion bombardment was applied to enhance the nucleation density of DNRs too. It was found that a bias of −100 V slightly decreases the nucleation density but greatly improves the size of individual spherules (see Figure 6b,d), being in contrast to bias enhanced nucleation of CVD diamond.

Another opposing habit on the nucleation and growth when compared to polycrystalline diamond, is that the nucleation density of DNRs on the scratched SiO_2 is higher than that on the scratched Si, as shown in Figure 6b,c. This could hint that the surface energy of substrates plays a minor role in determining the nucleation sites and mechanism of DNRs. The exact reason is not clear. It could be relevant to the release of oxygen from SiO_2 by the carbon-thermal reduction, leading to oxygen assisted 1D growth, similar to that met in other 1D nanomaterials,[38] because oxygen is able to replace hydrogen for the growth of highly crystalline diamond.[39] In contrast to carbon nanoflake and crystalline diamond,[27] no individual DNRs were found on the Si surface at the initial growth stage of several minutes. The growth of DNRs always proceeds in the form of spherules, accompanied with graphene nanowires and diamond nanoclusters. This could imply that the surface nanosteps formed by ion bombardment are not active nucleation sites for the DNR growth.[40] From the standpoint of vapor chemistry, the CH_3 and C_2H_2 radicals are considered as main growth species of diamond in an atomic hydrogen-rich ambient, while C_2 radicals are responsible for the growth of nanocrystalline diamond in an atomic hydrogen-poor environment. The growth of the present DNRs was carried out in a N_2-containing ambient, where CN and HCN radicals are dominant, implying that H_2 and Ar relevant radicals do

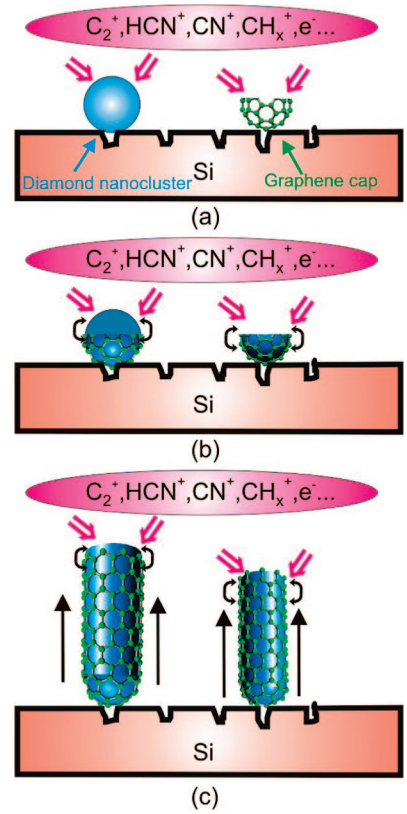

Figure 7. Schematic diagram of the growth model of ultrathin DNRs: (a) diamond nanocluster, curved graphene cap, and nano-onions preferentially nucleate on the scratched surface sites; (b) carbon radicals precipitate or adsorb on the surface of diamond nanoclusters and assemble themselves to form graphene/CNT caps. Alternatively, diamond nanoclusters nucleate on the curved graphene cap and nano-onions; (c) encapsulated diamond nanoclusters and outlayer graphenes/CNTs simultaneously start a 1D growth using the diamond nanocluster as catalysts.

not contribute to the growth of DNRs.[11,12] Another critical finding is ultrathin DNR was encapsulated in tapered CNTs, which could act as a high pressure reactive nanocell.[41] In this nanoscale cell, graphene curvature induces a surface tension effect or additional pressure, making diamond to be at a new thermodynamic stable region and to prefer to nucleate and grow on curved graphene planes inside the CNT.[42,43]

Here, we suggest that the growth of DNRs possibly follows a self-assembly mechanism as illustrated schematically in Figure 7. First, diamond nanoclusters together with nondiamond phases, such as the amorphous carbon, graphene cap, and nano-onion/nanowire simultaneously, nucleate preferentially at the scratched defect sites; Then, carbon radicals precipitate or adsorb on the surface of diamond nanoclusters, and assemble themselves to form graphene/CNT caps;[44] Finally, encapsulated diamond nanoclusters and outlayer graphenes/CNTs simultaneously start a 1D growth by a base catalytic growth mode *via* a phase separation, where the diamond nanoclusters are the solid catalysts.[45,46] This is a specific vapor-solid phase separation process yielding two carbon allotropes of diamond and graphene from the same carbon source, but different from the common self-catalytic growth, where there is only one final material product without phase separation. In this heterogeneous self-catalytic process, the diamond nanoclusters and outlayer graphenes start to grow from their interface at the same time, possibly like the in situ metal-filling CNT growth. Another possibility is that at the very beginning of growth a hemisphere graphene cap, fullerene, or a short CNT first forms on the surface and then diamond nucleates on the curved carbon cap due to the curvature induced surface tension effect. This can be evidenced by the presence of many fullerene and related materials, which were found to be one of precursors of both nanocrystalline diamond and CNTs.[47,48]

CONCLUSIONS

In conclusion, ultrathin DNRs were successfully grown on Si using a nitrogen-rich ambient in a MPCVD reactor. As-deposited DNRs have a length of 50−300 nm and a thin diameter of 2.1 nm, less than the theoretical minimum value for energetically stable DNRs. This was possible because they are encapsulated in tapered CNTs with an orientation relation of $(111)_{diamond}//(0002)_{graphite}$. The growth of DNRs is suggested to follow a heterogeneous self-catalytic vapor−liquid mechanism. DNRs were self-assembled with diamond nanoclusters, CNTs, and graphene nanowires/nano-onions into an integrated spherical nanostructure, leading to excellent field emission characteristics of low threshold and high current density due to the combined effect of all constituent nanomaterials. This new ultrathin DNR integrated nanostructure could offer opportunities for stimulating both future fundamental and experimental research with important applications in nanoelectronics and bioelectronics areas such as low-power cold cathodes and highly efficient and sensitive biosensors.

EXPERIMENTAL DETAILS

The growth of ultrathin DNRs was carried out in a 2.45 GHz, 1.5 kW microwave plasma enhanced CVD system. Clean (100) heavily doped n-type Si wafers with and without thermally oxidized SiO_2 coating were used as substrates. To enhance the nucleation density of diamond nanorods, the substrates were subjected to a standard surface pretreatment procedure that was used earlier for growing polycrystalline diamond films,[1] before being placed into the reaction chamber. A gas mixture of CH_4 and N_2 with a flowing ratio 5−30% was fed into the reactor. The total gas pressure and microwave power during the deposition were maintained at 20−60 torr and 700−1000 W, respectively. The growth lasted for 3−120 min. During deposition, the substrate was heated by a high-frequency induction coil up to 700−950 °C, as measured by an infrared optical pyrometer from the top window of the chamber. After deposition, the morphology and microstructure of the samples were characterized by SEM, TEM, STEM, and PEEM combined with NEXAFS spectroscopy. The NEXAFS spectroscopy at the C K-edge was collected at room temperature using an X-ray photoelectron energy microscope with a spatially lateral resolution of 30 nm in beamline I311 of the synchrotron radiation facility MAX-Laboratory (Lund, Sweden). STEM measurements were carried out in a 100 kV VGHB501 STEM retrofitted with a Nion Co. aberration corrector in SuperSTEM facility, Daresbury, U.K. Their field emission characteristics were investigated in vacuum at room temperature.

Acknowledgment. Authors thank S. Iyer and S. Sharma for their help in the preparation of some samples and the PEEM measurements. This work is financially supported by the European Union under the DESYGN-IT Project (STREP Project No. 505626), EPSRC funded facility access to SuperSTEM, and through Integrating Activity on Synchrotron and Free Electron Laser Program (IA-SFS No. RII3-CT-2004-506008).

REFERENCES AND NOTES

1. Lee, S. T.; Lin, Z. D.; Jiang, X. CVD Diamond Films: Nucleation and Growth. *Mater. Sci. Eng. R-Rep.* **1999**, *25*, 123–154.
2. Jorio, A.; Dresselhaus, G.; Dresselhaus, M. S. Carbon Nanotubes, Advanced Topics in the Synthesis, Structure, Properties and Applications Series. *Topics in Applied Physics*; Springer-Verlag GmbH: Berlin, 2008; Vol. 111.
3. Shenderova, O.; Brenner, D.; Ruoff, R. S. Would Diamond Nanorods be Stronger than Fullerene Nanotubes. *Nano Lett.* **2003**, *3*, 805–809.
4. Padgett, C. W.; Shenderova, O.; Brenner, D. W. Thermal Conductivity of Diamond Nanorods: Molecular Simulation and Scaling Relations. *Nano Lett.* **2006**, *6*, 1827–1831.
5. Fonoberov, V. A.; Balandin, A. A. Giant Enhancement of the Carrier Mobility in Silicon Nanowires with Diamond Coating. *Nano Lett.* **2006**, *6*, 2442–2446.
6. Ghosh, S.; Calizo, I.; Teweldebrhan, D.; Pokatilov, E. P.; Nika, D. L.; Balandin, A. A.; Bao, W.; Miao, F.; Lau, C. N. Extremely High Thermal Conductivity of Graphene: Prospects for Thermal Management Applications in Nanoelectronic Circuits. *Appl. Phys. Lett.* **2008**, *92*, 151911/1−151911/3.
7. Yang, N. J.; Uetsuka, H.; Osawa, E.; Nebel, C. E. Vertically Aligned Diamond Nanowires for DNA Sensing. *Angew. Chem., Int. Ed.* **2008**, *47*, 5183–5185.
8. Barnard, A. S.; Russo, S. P.; Snook, I. K. Electronic Band Gaps of Diamond Nanowires. *Phys. Rev. B* **2003**, *68*, 235407/1−235407/6.

9. Sun, L. T.; Gong, J. L.; Zhu, D. Z.; Zhu, Z. Y.; He, S. X. Diamond Nanorods from Carbon Nanotubes. *Adv. Mater.* **2004**, *16*, 1849–1852.
10. Dubrovinskaia, N.; Dubrovinsky, L.; Crichton, W.; Langenhorst, F.; Richter, A. Aggregated Diamond Nanorods, the Densest and Least Compressible Form of Carbon. *Appl. Phys. Lett.* **2005**, *87*, 83106/1−83106/3.
11. Vlasov, I. L.; Lebedev, O. I.; Ralchenko, V. G.; Goovaerts, E.; Bertoni, G.; Van Tendeloo, G.; Konov, V. I. Hybrid Diamond-Graphite Nanowires Produced by Microwave Plasma Chemical Vapor Deposition. *Adv. Mater.* **2007**, *19*, 4058–4062.
12. Arenal, R.; Bruno, P.; Miller, D. J.; Bleuel, M.; Lal, J.; Gruen, D. M. Diamond Nanowires and the Insulator-Metal Transition in Ultrananocrystalline Diamond Films. *Phys. Rev. B* **2007**, *75*, 195431/1−195431/11.
13. Masuda, H.; Yanagishita, T.; Yasui, K.; Nishio, K.; Yagi, I.; Rao, T. N.; Fujishima, A. Synthesis of Well-Aligned Diamond Nanocylinders. *Adv. Mater.* **2001**, *13*, 247–249.
14. Shenderova, O. A.; Padgett, C. W.; Hu, Z.; Brenner, D. W. Diamond Nanorods. *J. Vac. Sci. Technol. B* **2005**, *23*, 2457–2464.
15. Zou, Y. S.; Yang, Y.; Zhang, W. J.; Chong, Y. M.; He, B.; Bello, I.; Lee, S. T. Fabrication of Diamond Nanopillars and Their Arrays. *Appl. Phys. Lett.* **2008**, *92*, 53105/1−53105/3.
16. Barnard, A. S.; Snook, I. K. Phase Stability of Nanocarbon in One Dimension: Nanotubes *versus* Diamond Nanowires. *J. Chem. Phys.* **2004**, *120*, 3817–3821.
17. Barnard, A. S.; Russo, S. P.; Snook, I. K. *Ab Initio* Modeling of Diamond Nanowire Structures. *Nano Lett.* **2003**, *3*, 1323–1328.
18. Sun, C.; Zhang, W. J.; Wang, N.; Chan, C. Y.; Bello, I.; Lee, C. S.; Lee, S. T. Crystal Morphology and Phase Purity of Diamond Crystallites During Bias Enhanced Nucleation and Initial Growth Stages. *J. Appl. Phys.* **2000**, *88*, 3354–3360.
19. Shang, N. G.; Staedler, T.; Jiang, X. Radial Textured Carbon Nanoflake Spherules. *Appl. Phys. Lett.* **2006**, *89*, 103112/1−103112/3.
20. Wang, P.; Bleloch, A. L.; Falke, U.; Goodhew, P. J. Three-Dimensional Reconstruction of Au Nanoparticles Using Five Projections from an Aberration-Corrected STEM. *Ultramicroscopy* **2006**, *106*, 277–283.
21. Wang, P; D'Alfonso, A J; Findlay, S D; Allen, L J; Bleloch, A L. Contrast Reversal in Atomic-Resolution Chemical Mapping. *Phys. Rev. Lett.* **2008**, *101*, 236102/1−236102/4.
22. Lambrecht, W. R. L.; Lee, C. H.; Segall, B.; Angus, J. C.; Li, Z. D.; Sunkara, M. Diamond Nucleation by Hydrogenation of the Edges of Graphitic Precusors. *Nature (London)* **1993**, *364*, 607–610.
23. Chang, Y. K.; Hsieh, H. H.; Pong, W. F.; Tsai, M. H.; Chien, F. Z.; Tseng, P. K.; Chen, L. C.; Wang, T. Y.; Chen, K. H.; Bhusari, D. M.; Yang, J. R.; Lin, S. T. Quantum Confinement Effect in Diamond Nanocrystals Studied by X-ray-Absorption Spectroscopy. *Phys. Rev. Lett.* **1999**, *82*, 5377–5380.
24. Birrell, J.; Gerbi, J. E.; Auciello, O.; Gibson, J. M.; Gruen, D. M.; Carlisle, J. A. Bonding Structure in Nitrogen Doped Ultrananocrystalline Diamond. *J. Appl. Phys.* **2003**, *93*, 5606–5612.
25. Tzeng, Y. F.; Lee, Y. C.; Lee, C. Y.; Lin, I. N.; Chiu, H. T. On the Enhancement of Field Emission Performance of Ultrananocrystalline Diamond Coated Nanoemitters. *Appl. Phys. Lett.* **2007**, *91*, 063117/1−063117/3.
26. Shang, N. G.; Papakonstantinou, P.; McLaughlin, J.; Chen, W. C.; Chen, L. C.; Chu, M.; Stamboulis, A. Fe Catalytic Growth, Microstructure, and Low-Threshold Field Emission Properties of Open Ended Tubular Graphite Cones. *J. Appl. Phys.* **2008**, *103*, 124308/1−124308/2.
27. Shang, N. G.; Au, F. C. K.; Meng, X. M.; Lee, C. S.; Bello, I.; Lee, S. T. Uniform Carbon Nanoflake Films and Their Field Emissions. *Chem. Phys. Lett.* **2002**, *358*, 187–191.
28. Shang, N. G.; Li, C. P.; Wong, W. K.; Lee, C. S.; Bello, I.; Lee, S. T. Microstructure and Field Emission Properties of Coral-like Carbon Nanotubes. *Appl. Phys. Lett.* **2002**, *81*, 5024–5026.
29. Yang, Y. H.; Wang, B.; Xu, N. S.; Yang, G. W. Field Emission of One-Dimensional Micro- and Nanostructures of Zinc Oxide. *Appl. Phys. Lett.* **2006**, *89*, 043108/1−043108/3.
30. Zhu, W.; Bower, C.; Zhou, O.; Kochanski, G.; Jin, S. Large Current Density from Carbon Nanotube Field Emitters. *Appl. Phys. Lett.* **1999**, *75*, 873–875.
31. Zhu, W.; Kochanski, G. P.; Jin, S. Low-Field Electron Emission from Undoped Nanostructured Diamond. *Science* **1998**, *282*, 1471–1473.
32. Tarntair, F. G.; Chen, L. C.; Wei, S. L.; Hong, W. K.; Chen, K. H.; Cheng, H. C. High Current Density Field Emission from Arrays of Carbon Nanotubes and Diamond-Clad Si Tips. *J. Vac. Sci. Technol. B* **2000**, *18*, 1207–1211.
33. Rao, A. M.; Jacques, D.; Haddon, R. C.; Zhu, W.; Bower, C.; Jin, S. In Situ-Grown Carbon Nanotube Array with Excellent Field Emission Characteristics. *Appl. Phys. Lett.* **2000**, *76*, 3813–3815.
34. Cui, J. B.; Stammler, M.; Ristein, J.; Ley, L. Role of Hydrogen on Field Emission from Chemical Vapor Deposited Diamond and Nanocrystalline Diamond Powder. *J. Appl. Phys.* **2000**, *88*, 3667–3673.
35. Cui, J. B.; Ristein, J.; L., Ley. Electron Affinity of the Bare and Hydrogen Covered Single Crystal Diamond (111) Surface. *Phys. Rev. Lett.* **1998**, *81*, 429–432.
36. Gruen, D. M. Nanocrystalline Diamond Films. *Annu. Rev. Mater. Sci.* **1999**, *29*, 211–259.
37. Zhu, Z. P.; Lu, Y.; Qiao, D. H.; Bai, S. L.; Hu, T. P.; Li, L.; Zheng, J. F. Self-Catalytic Behavior of Carbon Nanotubes. *J. Am. Chem. Soc.* **2005**, *127*, 15698–15699.
38. Zhang, R. Q.; Lifshitz, Y.; Lee, S. T. Oxide-Assisted Growth of Semiconducting Nanowires. *Adv. Mater.* **2003**, *15*, 635–640.
39. Yoshimoto, M.; Yoshida, K.; Maruta, H.; Hishitani, Y.; Koinuma, H.; Nishio, S.; Kakihana, M.; Tachibana, T. *Nature (London)* **1999**, *399*, 340–342.
40. Lee, S. T.; Peng, H. Y.; Zhou, X. T.; Wang, N.; Lee, C. S.; Bello, I.; Lifshitz, Y. A Nucleation Site and Mechanism Leading to Epitaxial Growth of Diamond Films. *Science* **2000**, *287*, 104–106.
41. Sun, L.; Banhart, F.; Krasheninnikov, A. V.; Rodríguez-Manzo, J. A.; Terrones, M.; Ajayan, P. M. Carbon Nanotubes as High-Pressure Cylinders and Nanoextruders. *Science* **2006**, *312*, 1199–1202.
42. Wang, C. X.; Yang, Y. H.; Xu, N. S.; Yang, G. W. Thermodynamics of Diamond Nucleation on the Nanoscale. *J. Am. Chem. Soc.* **2004**, *126*, 11303–11306.
43. Liu, Q. X.; Wang, C. X.; Li, S. W.; Zhang, J. X.; Yang, G. W. Nucleation Stability of Diamond Nanowires inside Carbon Nanotubes: A Thermodynamic Approach. *Carbon* **2004**, *42*, 629–633.
44. Takagi, D.; Hibino, H.; Suzuki, S.; Kobayashi, Y.; Homma, Y. Carbon Nanotube Growth from Semiconductor Nanoparticles. *Nano Lett.* **2007**, *7*, 2272–2275.
45. Gavillet, J; Loiseau, A.; Journet, C.; Willaime, F.; Ducastelle, F.; Charlier, J. C. Root-Growth Mechanism for Single-Wall Carbon Nanotubes. *Phys. Rev. Lett.* **2001**, *87*, 275504/1−275504/4.
46. Hofmann, S.; Sharma, R.; Ducati, C.; Du, G.; Mattevi, C.; Cepek, C.; Cantoro, M.; Pisana, S.; Parvez, A.; Cervantes-Sodi, F.; Ferrari, A. C.; Dunin-Borkowski, R.; Lizzit, S.; Petaccia, L.; Goldoni, A.; Robertson, J. *In Situ* Observations of Catalyst Dynamics during Surface-Bound Carbon Nanotube Nucleation. *Nano Lett.* **2007**, *7*, 602–608.
47. Pfeiffer, R.; Holzweber, M.; Peterlik, H.; Kuzmany, H.; Liu, Z.; Suenaga, K.; Kataura, H. Dynamics of Carbon Nanotube Growth from Fullerenes. *Nano Lett.* **2007**, *7*, 2428–2434.
48. Gruen, D. M. *Perspective of Fullerene Nanotechnology;* Springer: The Netherlands, 2002; Part V, pp 217−222.